Supplementary Figures

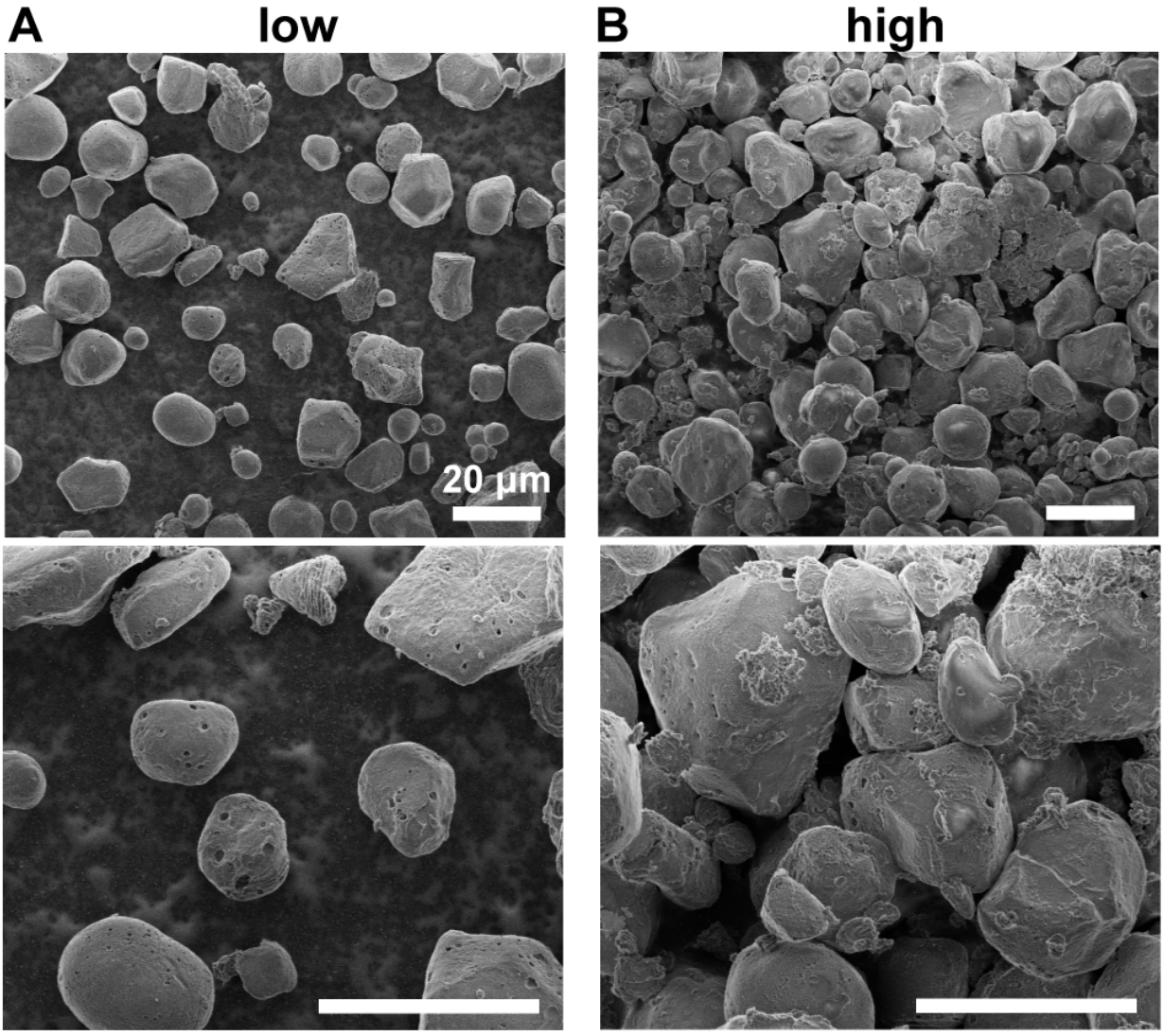

Fig. S1. Starch degradation with different VAL-0417:starch ratios, related to Figure 1. (A) Degradation with low ratio (10 µg VAL-0417, 1 mg starch). (B) Degradation with high ratio (10 µg VAL-0417, 100 µg starch).

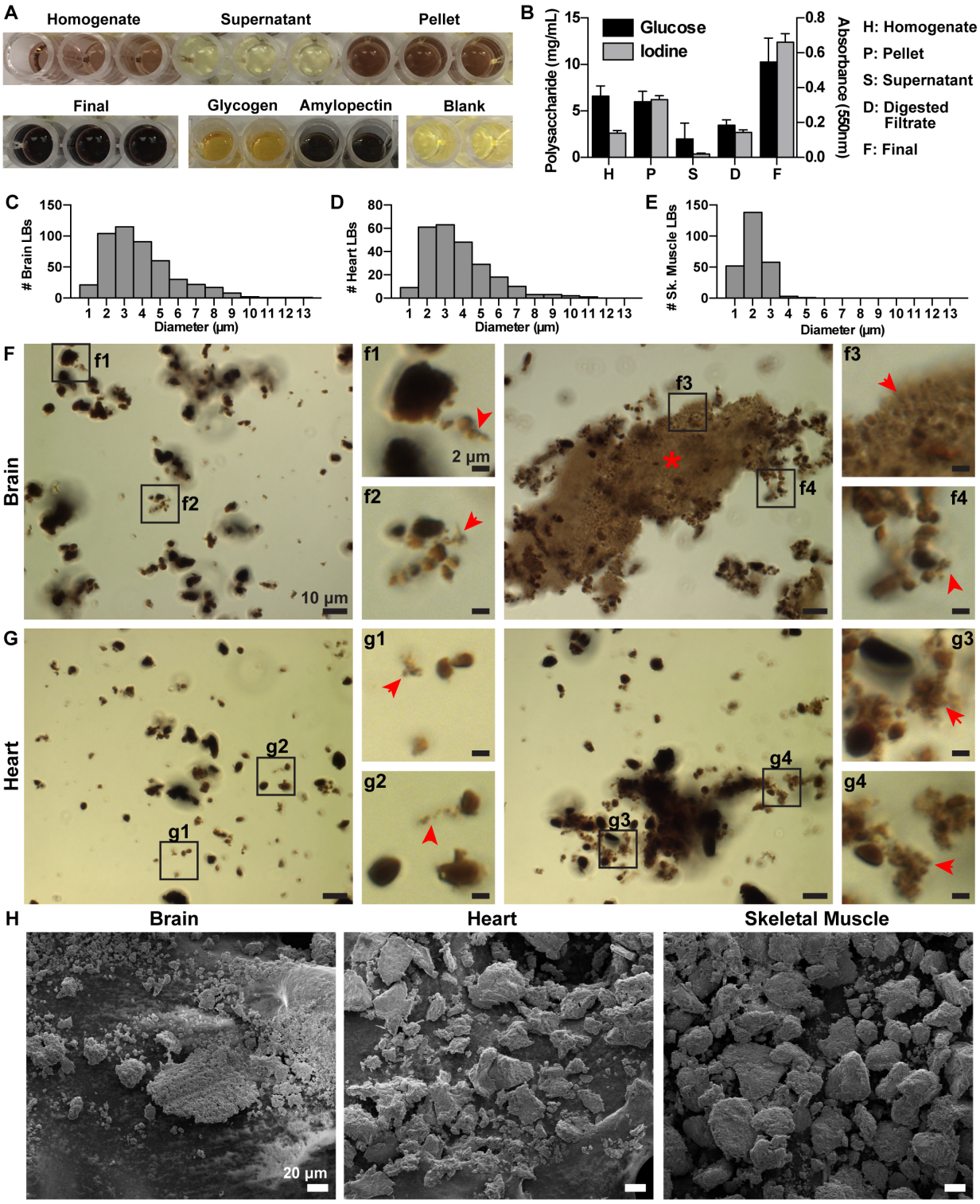

Fig. S2. Iodine staining and appearance of native LBs, related to Figures 2 and 3. (A) 50 μL samples were removed from homogenate, supernatant, and pellet fractions during preliminary LB purifications from skeletal muscle, boiled for 30 minutes, and clarified by centrifugation. 30 μL of the clarified sample was diluted with 15 μL water and stained with 50 μL 1x Lugol's

solution in a microplate. Commercial liver glycogen and amylopectin were also stained as controls. (B) Concentration vs. iodine absorbance at 550 nm of Pflüger-isolated polysaccharide from skeletal muscle at each step of the purification scheme. (C,D,E) Frequency distribution of LBs from each tissue type: (C) brain (total count: 473), (D) heart (total count: 247), and (E) skeletal muscle (total count: 252). (F,G) Two fields of view from (F) brain and heart (G) LB preparations containing numerous dust-like particles are shown. Black boxes indicate areas that have been magnified and are labeled correspondingly (f1, f2, etc.). Occasionally very large bodies were observed (10-20 µm). They were difficult to distinguish from tightly packed clumps, so they were excluded from the size distribution histograms. (H) Scanning electron micrographs of LBs from brain, heart and skeletal muscle, washed in ethanol, dried, and applied to carbon tape (See STAR Methods). Samples were visualized at 2kV under high vacuum by an FE Quanta 250.

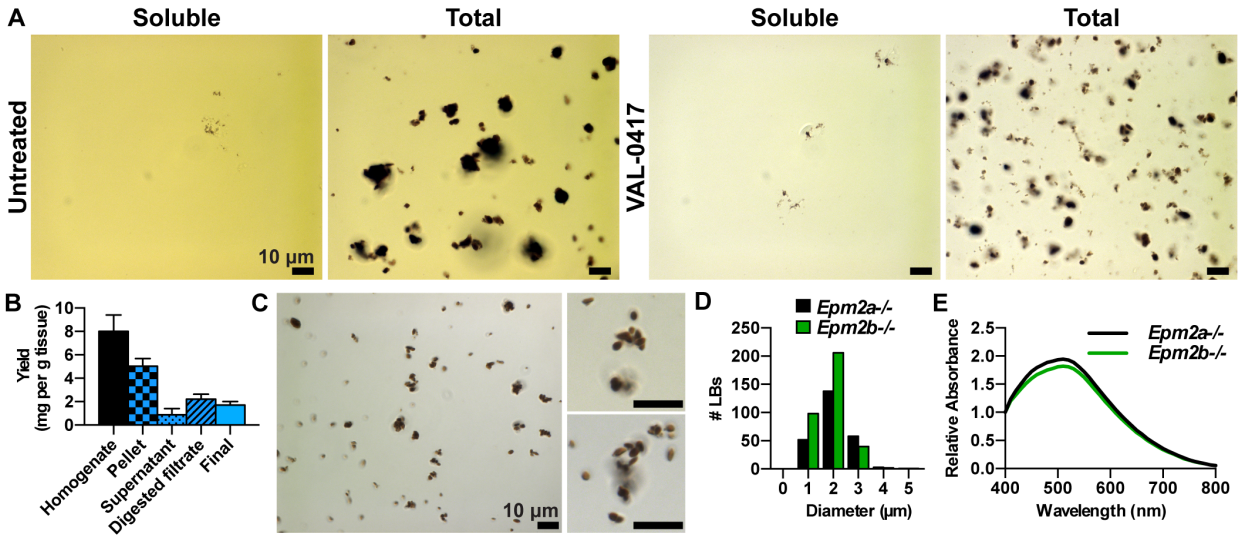

Fig. S3. Soluble fractions of untreated and treated brain LBs (BrLBs) and purification of *Epm2b-/-* LBs from skeletal muscle, related to Figure 4. (A) Samples from the soluble fractions and total reactions were stained with Lugol's solution and visualized using a Zeiss Axioimager Z1. (B) *Epm2b-/-* LB purification yields. Mean ± SD of triplicate measurements are shown. (C) *Epm2b-/-* LBs stained with Lugol's solution and visualized by light microscopy. (D) Comparison of size distribution of skeletal muscle LBs from *Epm2a-/-* and *Epm2b-/-* mice. (E) Normalized iodine spectra of *Epm2b-/-* and *Epm2a-/-* skeletal muscle LBs. The spectral data are an average of 3 replicates.

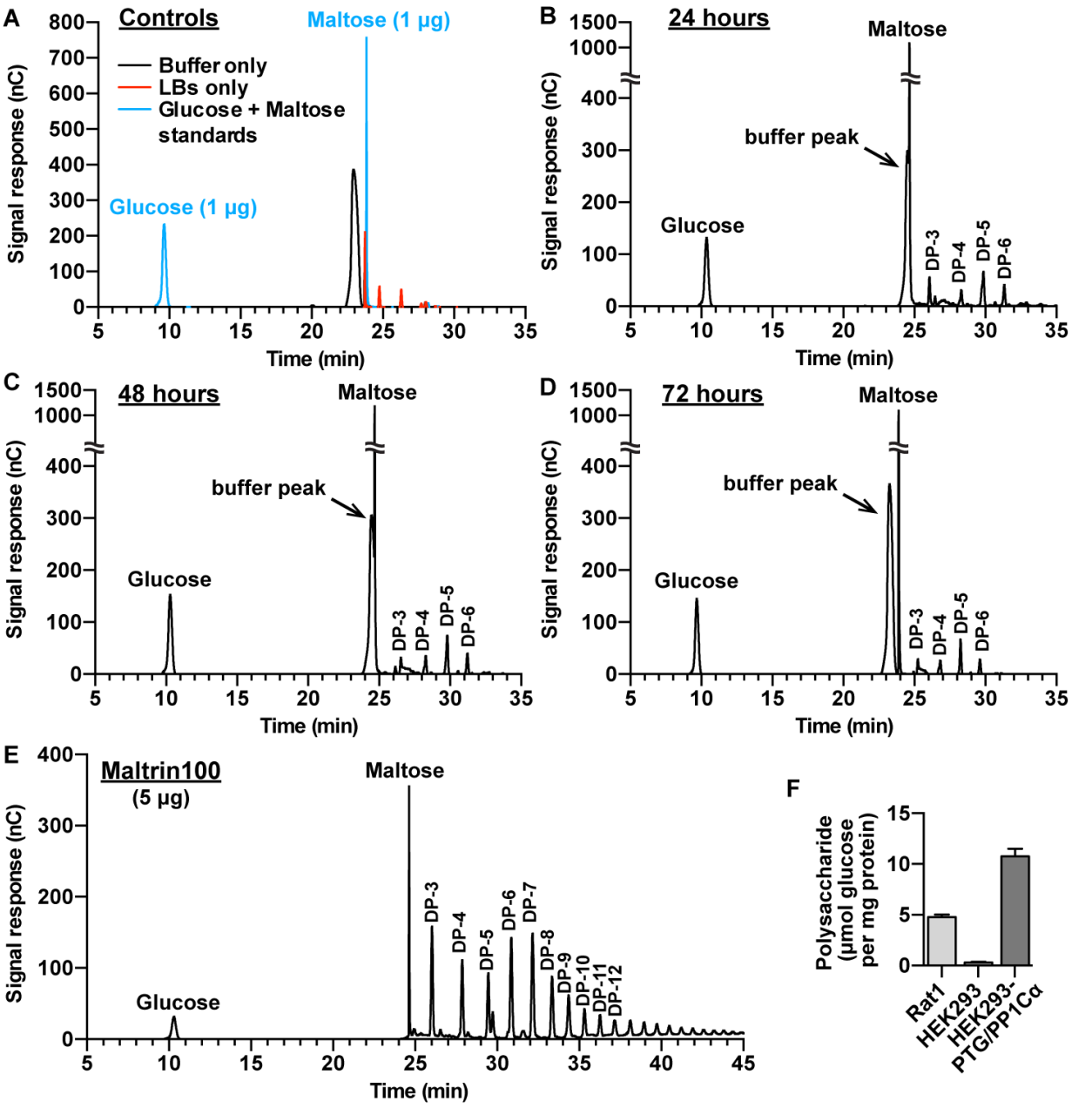

Fig. S4. HPAEC-PAD chromatograms from LB degradation by VAL-0417 *in vitro*, related to Figure 4, and polysaccharide levels in three cell lines, related to Figure 5. (A) Overlay of control chromatograms: degradation buffer only (black line), LBs only (red line), and a mixture of 1 µg glucose and 1 µg maltose standards for quantitation (blue line). A small amount of maltose and low molecular weight oligosaccharides were detected in the LB control. Additional time points from the 168 hour LB degradation experiment with VAL-0417: (B) 24 hours, (C) 48 hours, and (D) 72 hours. Each chromatogram is representative of triplicate chromatograms. Small shifts in retention time (≤1 min) are typical between HPAEC-PAD runs. (E) Maltrin100, a mixture of low molecular weight oligosaccharides, was used as a standard for verifying degrees of polymerization (DP), i.e. number of glucose units. (F) Polysaccharide levels relative to protein

concentration in three cell lines: Rat1, HEK293, and HEK293 stably expressing PTG and PP1Cα, related to Figure 5. Data are expressed as the mean of 12 replicates ± SE.

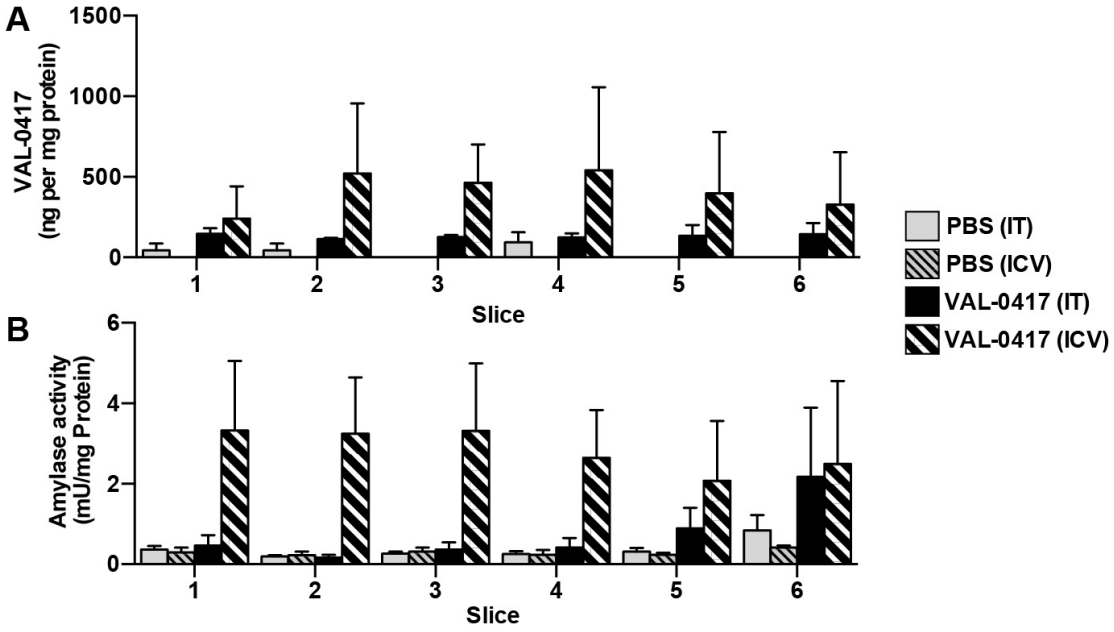

Fig. S5. Comparison of intrathecal (IT) versus intracerebroventricular (ICV) routes of administration in WT mice, related to Figure 7. (A) Distribution of VAL-0417 levels using the sandwich ELISA in PBS- and VAL-0417-treated WT brain slices after intrathecal (IT) or intracerebroventricular (ICV) infusion. (B) Distribution of VAL-0417 activity in the same slices measured using the BioVision amylase activity assay. Data shown are a mean of 3 measurements ± SE.

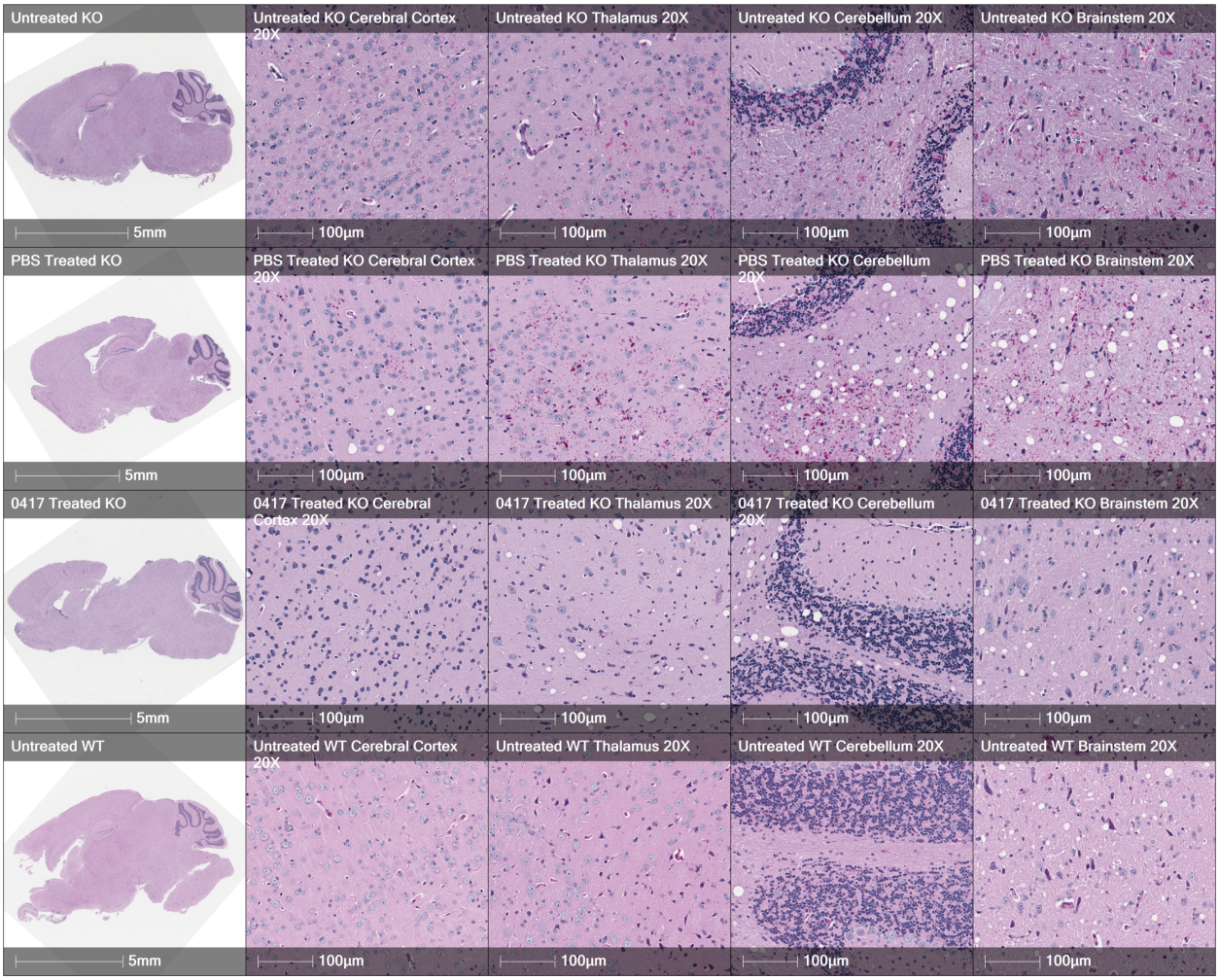

Fig. S6. Regional distribution of LB load in PBS and VAL-0417 treated *Epm2a-/-* (KO) animals compared to untreated WT and *Epm2a-/-* controls, related to Figure 7. PAS-stained slides were counterstained with hematoxylin (blue). LBs appear as PAS+ inclusions (bright purple). Slides were scanned and images were prepared using the HALO software (PerkinElmer). The left column represents the entire slice at low magnification; the other columns show individual regions at higher magnification and are labeled accordingly. Brain slices are representative of all animals analyzed for each group.

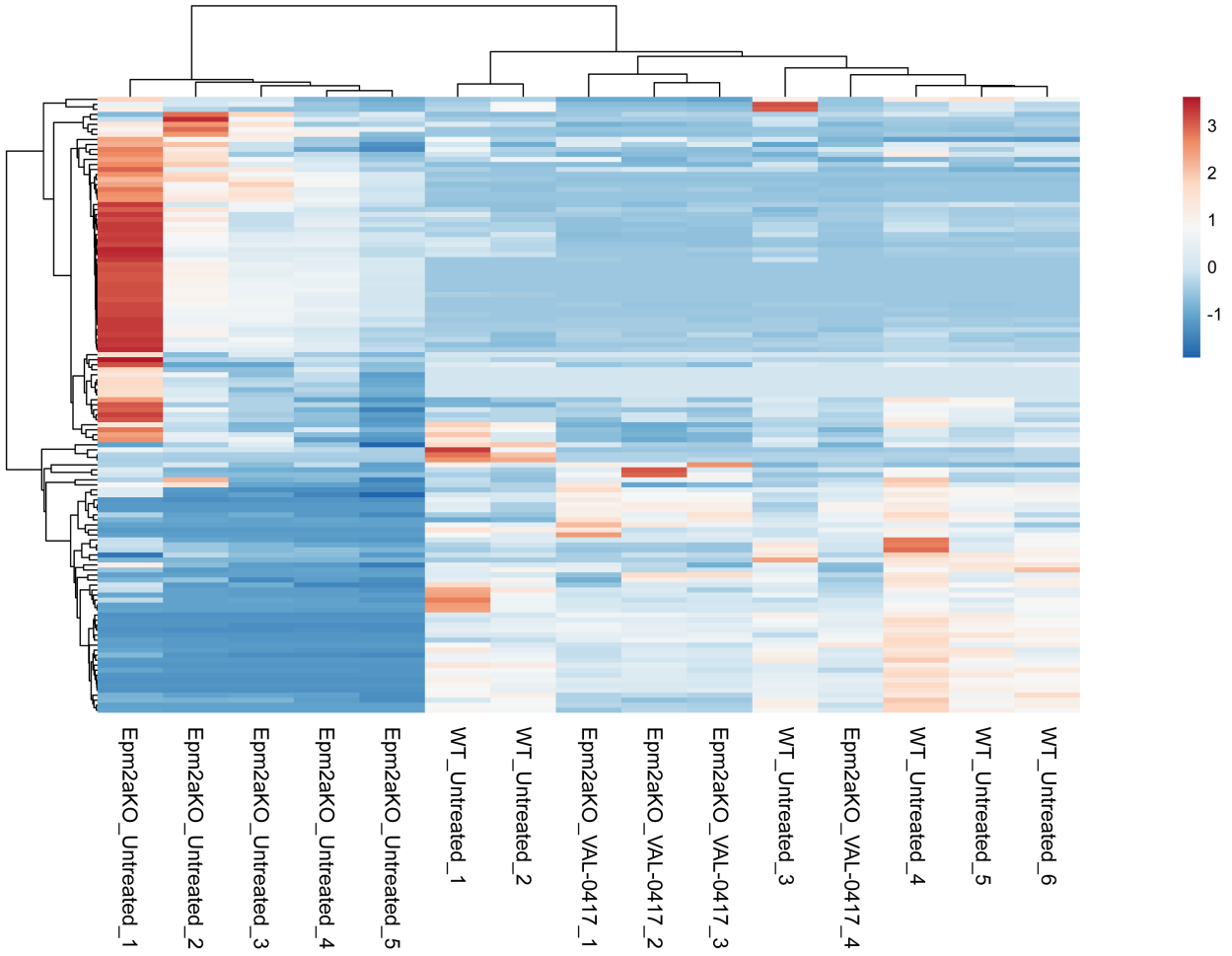

Fig. S7. Clustering heat map analysis illustrating the similarities in metabolite profiles between untreated WT and *Epm2a-/-* mice treated with VAL-0417 compared to PBS treated *Epm2a-/-* (KO) mice, related to Figure 7. Each row represents a metabolite, while each column represents an individual mouse. Colors indicate the magnitude of the difference between groups (log_2 transformed relative abundance). The PBS-treated *Epm2a-/-* group was omitted to prevent confounding the groups.